

# Journal of Composite Materials

<http://jcm.sagepub.com/>

---

## **Thermo-mechanical properties of acrylated epoxidized hemp oil based biocomposites**

NW Manthey, F Cardona, G Francucci and T Aravinthan

*Journal of Composite Materials* 2014 48: 1611 originally published online 17 May 2013

DOI: 10.1177/0021998313488155

The online version of this article can be found at:

<http://jcm.sagepub.com/content/48/13/1611>

---

Published by:



<http://www.sagepublications.com>

On behalf of:



[American Society for Composites](http://www.americansocietyforcomposites.com)

**Additional services and information for *Journal of Composite Materials* can be found at:**

**Email Alerts:** <http://jcm.sagepub.com/cgi/alerts>

**Subscriptions:** <http://jcm.sagepub.com/subscriptions>

**Reprints:** <http://www.sagepub.com/journalsReprints.nav>

**Permissions:** <http://www.sagepub.com/journalsPermissions.nav>

**Citations:** <http://jcm.sagepub.com/content/48/13/1611.refs.html>

>> [Version of Record](#) - May 15, 2014

[OnlineFirst Version of Record](#) - May 17, 2013

[What is This?](#)

# Thermo-mechanical properties of acrylated epoxidized hemp oil based biocomposites

NW Manthey<sup>1</sup>, F Cardona<sup>1</sup>, G Francucci<sup>1,2</sup> and T Aravinthan<sup>1</sup>

## Abstract

In this study, novel acrylated epoxidized hemp oil bioresin was used in the manufacturing of jute fibre reinforced biocomposites. The 100% biocomposite laminates were characterised in terms of mechanical properties (tensile, flexural, Charpy impact and interlaminar shear), thermo-mechanical properties (glass transition temperature, storage modulus and crosslink density) and water absorption properties (saturation moisture level and diffusion coefficient). Comparisons with the equivalent synthetic vinylester resin based jute fibre reinforced biocomposite panels were performed. Scanning electron microscopic analysis confirmed panel samples containing acrylated epoxidized hemp oil to display improved fibre–matrix interfacial adhesion compared with the vinylester resin based samples. Furthermore in terms of mechanical properties acrylated epoxidized hemp oil based biocomposites compared favourably with those manufactured from vinylester resin synthetic resin. Dynamic mechanical analysis found acrylated epoxidized hemp oil based biocomposites to have lower glass transition temperature, storage modulus and crosslink density than vinylester resin based samples. Increasing acrylated epoxidized hemp oil content resulted in a marginal increase in saturation moisture content and diffusion coefficient.

## Keywords

Acrylated epoxidized hemp oil, biocomposite, hemp oil, mechanical properties, scanning electron microscope

## Introduction

In the search for high performance construction materials, fibre composites are now being more widely utilised than in the past. Fibre composites generally use petrochemically derived polymer resins for example; epoxy, polyester and vinylester because of their advantageous material properties such as high stiffness and strength properties. However, these resins also have serious shortcomings in terms of biodegradability, initial processing cost, recyclability, energy consumption and processing health hazards. Increasing environmental awareness throughout society and now within the civil engineering and construction industries is driving the research, development and utilisation of more ‘green’ building materials, specifically the development of bioresins and biocomposites based on renewable, natural materials.

Plant-oil-based bioresins are an emerging ‘green’ thermoset material and due to their biological origin they represent a sustainable, low environmental

impact option to existing petrochemically derived resins. These plant-oil-based bioresins may be reinforced with natural or synthetic fibres thereby creating a class of materials termed, natural fibre composites or biocomposites. Currently a high proportion of biocomposites are being produced using petrochemical-based matrices reinforced with natural fibres.<sup>1–8</sup> However, these composites may more aptly be termed hybrid composites as they contain both natural and synthetic constituents.

<sup>1</sup>Centre of Excellence in Engineered Fibre Composites (CEEFC), University of Southern Queensland, Australia

<sup>2</sup>Composite Materials Group, Research Institute of Material Science and Technology (INTEMA-CONICET), Materials Engineering Department, Engineering Faculty, National University of Mar del Plata, Argentina

## Corresponding author:

NW Manthey, Centre of Excellence in Engineered Fibre Composites (CEEFC), University of Southern Queensland, Toowoomba, Queensland, Australia.

Email: nathan.manthey@usq.edu.au

In terms of an environmental perspective it is imperative to produce composites in which both the matrix and fibre reinforcement are derived from natural resources thereby fostering sustainability. Natural materials such as plant-based bioresin and fibres have low environmental impact given that they are natural in origin and are therefore a suitable renewable resource from which biocomposites are produced. In this study, a thermosetting hemp oil based bioresin, acrylated epoxidized hemp oil (AEHO) was synthesised and applied to the manufacturing of jute mat reinforced 100% biocomposites.

Composite panels containing AEHO bioresin, blends of 50/50 (vinyl ester (VE)/AEHO) and synthetic VE resin with jute fibre mat reinforcement were manufactured by the hand lay-up technique. Mechanical properties (tensile, flexural, Charpy impact and interlaminar shear), thermo-mechanical properties (glass transition temperature, storage modulus and crosslink density) and water absorption properties (saturation moisture level and diffusion coefficient) were investigated and compared with the composite samples with the three different type of resin used as the polymeric matrix in this work.

## Materials

AEHO as synthesised according to our previous publications and containing 4.1 acrylate and hydroxyl groups per triglyceride was used as the base bioresin.<sup>9,10</sup> FG vinylester SPV6003 (FGI Australia) was used as received for the control samples. In the case of the AEHO bioresin, the added styrene comonomer was supplied by Fischer Scientific (UK), the Promoter N2-51P was sourced from Axon Nobel Ltd and a 40% MEKP-based catalyst was used for the curing and sourced from FGI Australia. The Styrene comonomer, promoter and catalyst were all used as received. Woven jute fibre, 90°/0°, 550 g/m<sup>2</sup> was used as natural fibre reinforcement.

## Experimental

### Sample preparation

To prepare the AEHO bioresin, 33 wt% of styrene was added in order to decrease viscosity and improve processability for manufacturing composite parts by traditional composite processing techniques. Afterwards, the promoter was incorporated to the AEHO/styrene mixture (0.25 wt%) and thoroughly mixed. Subsequently the catalyst was added (4 wt%) and stirred thoroughly for several minutes. The resin was degassed under vacuum. Both VE and 50/50 (VE/AEHO) were prepared following a similar method.

However, for the VE resin system no styrene was added as the system already contained 33 wt% of styrene. Regarding the VE system, 0.25% and 2% promoter and catalyst were used, respectively. For the 50/50 (VE/AEHO) system 0.25% and 3% promoter and catalyst were used, respectively. Neat bioresin and resin samples were also produced by pouring into a waxed glass mould.

Biocomposite panels were manufactured using the hand lay-up process consisting of four layers of woven jute mat reinforcement. The fibre was cut to size, washed with warm water to remove any dust particles and other such contaminants and was dried for 12 h at 110°C. No chemical treatments were performed on the fibre. The manufacture of the composite panels was performed immediately upon removing the fibre from the oven to prevent atmospheric moisture absorption which could impinge upon the final composite's mechanical properties. Three different sample types were prepared: namely VE + jute fibre, 50/50 (VE/AEHO) + jute fibre and AEHO + jute fibre. Manufactured panels were 300 × 300 × 5 mm<sup>3</sup> with a fibre weight percentage of approximately 25%.

Initial curing for both bioresin and biocomposite samples was performed at room temperature (~25°C) for 4 h followed by a 4 h post curing stage performed at 80°C for the vinylester and at 120°C for the bioresin composites to achieve maximum curing (100%). Following this the samples were removed from the moulds, cut to size, dried at 80°C for 4 h to ensure the removal of any induced moisture and then cooled in a desiccator ready for testing. An exception to this process was that the water absorption samples were further dried at 110°C for 1 h and cooled in a desiccator as per ASTM D570.

### Scanning electron microscopy

Cross-section morphologies of the biocomposite samples were investigated with a JEOL JSM 6460 LV scanning electron microscope (SEM) at National University of Mar Del Plata, Argentina (UNMdP). The fractured surfaces were coated with gold and the samples were scanned at room temperature with an accelerating voltage of 15 kV.

### Mechanical testing

Interlaminar shear strength (ILSS) testing was performed to determine the effects of bioresin concentration on the fibre-matrix interfacial shear strength. Testing was performed using ISO 14130 on a MTS Alliance RT/10 10 kN machine with a crosshead speed of 1 mm/min. Five specimens of each sample type were used in each mechanical test. Charpy

impact tests were conducted to determine the effects of bioresin concentration on the impact properties of the biocomposites. Impact properties of the samples were determined using ISO 179 on an Instron Dynatup M14-5162. Charpy impact strength ( $\text{kJ/m}^2$ ) was calculated from equation (1), whereby  $a_{cU}$ ,  $h$ ,  $b$  an  $W_B$  are the Charpy impact strength, thickness, width and the energy at break of the test specimen, respectively. Essentially Charpy impact strength corresponds to the energy at break of the specimen divided by the cross-sectional area.

$$a_{cU} = \frac{W_B}{bh} \times 10^3 \quad (1)$$

Flexural testing was conducted to determine the behaviour of both bioresin and biocomposite specimens subjected to 3-point simple beam loading. Bioresin flexural properties were obtained through 3-point bending tests conducted in accordance with ISO 178 using a MTS Alliance RT/10 machine. A cross-head speed of 2 mm/min and a span/depth ratio of 16:1 were used with specimen dimensions being  $80 \times 10 \times 5 \text{ mm}^3$ . Biocomposite flexural properties were measured in accordance with ISO 14125. Tensile tests were conducted in accordance with ISO 527. Tests were performed with a cross-head speed of 2 mm/min using a MTS Insight 100 kN machine. Specimen dimensions were  $250 \times 25 \times 5 \text{ mm}^3$ .

### Dynamic mechanical analysis

A calibrated TA Instruments Q800 DMA was used for the dynamic mechanical analysis (DMA). Rectangular specimens with the dimensions  $58 \times 10 \times 4 \text{ mm}^3$  were tested in dual cantilever mode. Testing was performed at a temperature ramp of  $3^\circ\text{C}/\text{min}$  over a temperature range of approximately  $25\text{--}180^\circ\text{C}$ . A frequency of 1.0 Hz with an oscillating displacement of  $\pm 10 \mu\text{m}$  was also used. Storage modulus ( $E'$ ) and  $\tan \delta$  were plotted as a function of temperature by Universal Analysis 2000 version 3.9A software. Glass transition temperature ( $T_g$ ) was calculated as the peak of the  $\tan \delta$  curve and crosslink density ( $\nu_e$ ) was calculated from the theory of rubber elasticity<sup>11</sup>

$$E' = 3\nu_e RT \quad (2)$$

Here  $E'$ ,  $\nu_e$ ,  $R$  and  $T$  are the storage modulus in the rubbery plateau region ( $T_g + 40^\circ\text{C}$ ), crosslink density, gas constant ( $8.314 \text{ J}/(\text{K}\cdot\text{mol})$ ) and the absolute temperature in K, respectively.<sup>12</sup>

### Moisture absorption

Moisture absorption tests were performed in order to ascertain the saturation moisture level and the diffusion

coefficient of the bioresin and biocomposite samples. Specifically the effects of bioresin loading on the moisture absorption properties were of interest. Testing was performed in accordance with ASTM D570. Specimens measured  $76.2 \times 25.4 \times 5 \text{ mm}^3$  for both neat resin and biocomposite samples. Three specimens of each sample type were used. The specimens were cut to size and the edges were finished with No. 0 sandpaper. After this the specimens were dried at  $110^\circ\text{C}$  for 1 h, cooled in a desiccator and weighed to the nearest 0.001 g. The specimens were immersed in distilled water at  $23 \pm 1^\circ\text{C}$  and removed at regular intervals, wiped free of surface moisture, immediately weighed to the nearest 0.001 g and then replaced in the water. Equation (3) was used to calculate the diffusion coefficient.

$$D = \pi \left( \frac{h}{4M_m} \right) m^2 \quad (3)$$

Here  $D$ ,  $h$ ,  $M_m$  and  $m$  are diffusion coefficient, thickness of specimen, saturation moisture level and gradient of the linear region from the plot of weight gain against square root of time, respectively.<sup>13</sup>

## Results and discussion

### SEM analysis

In fibre composites effective wetting and compatibility between the fibre reinforcement and the polymer matrix is paramount in obtaining satisfactory fibre–matrix adhesion and ultimately acceptable end state composite properties. SEM micrographs of both epoxidized and acrylated samples were taken to investigate the fibre–matrix interfaces.

Specifically, the fracture surfaces of the VE, 50/50 (VE/AEHO) and AEHO-based jute fibre reinforced samples were examined by SEM to evaluate the degree of fibre–matrix adhesion. Magnification of  $300\times$  was used to give a representative image of the overall fibre–matrix behaviour whereas  $1000\times$  magnification was used to more closely examine individual fibre–matrix behaviour.

Figures 1 to 6 display the typical fibre–matrix interface of all three different sample types. Fibre pullout is evident for all sample types and is visible at  $300\times$  magnification. Also apparent is the fibre–matrix interface and the presence of some gaps between the fibre and the matrix. Indeed this fibre–matrix interface condition was anticipated as no chemical treatment was performed on the jute fibre reinforcement. Samples containing 100% VE were observed to have the poorest fibre–matrix interface, with the 100% AEHO samples displaying improved fibre–matrix adhesion. It is proposed that the superior fibre–matrix interfacial



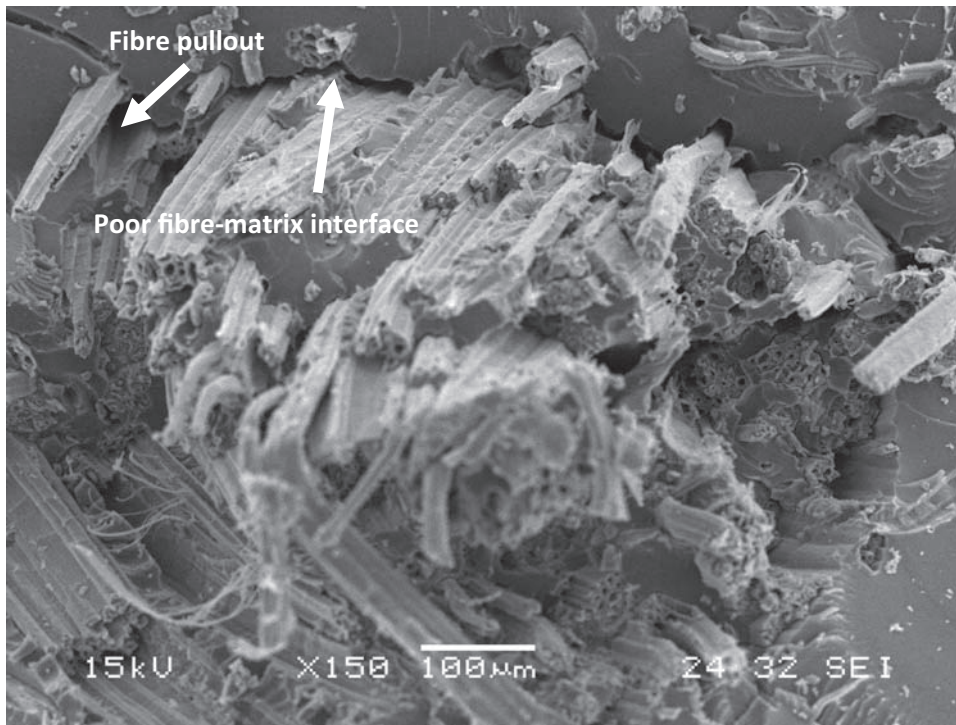


**Figure 1.** SEM micrograph of synthetic vinylester reinforced jute fibre biocomposite.  
SEM: scanning electron microscopy.

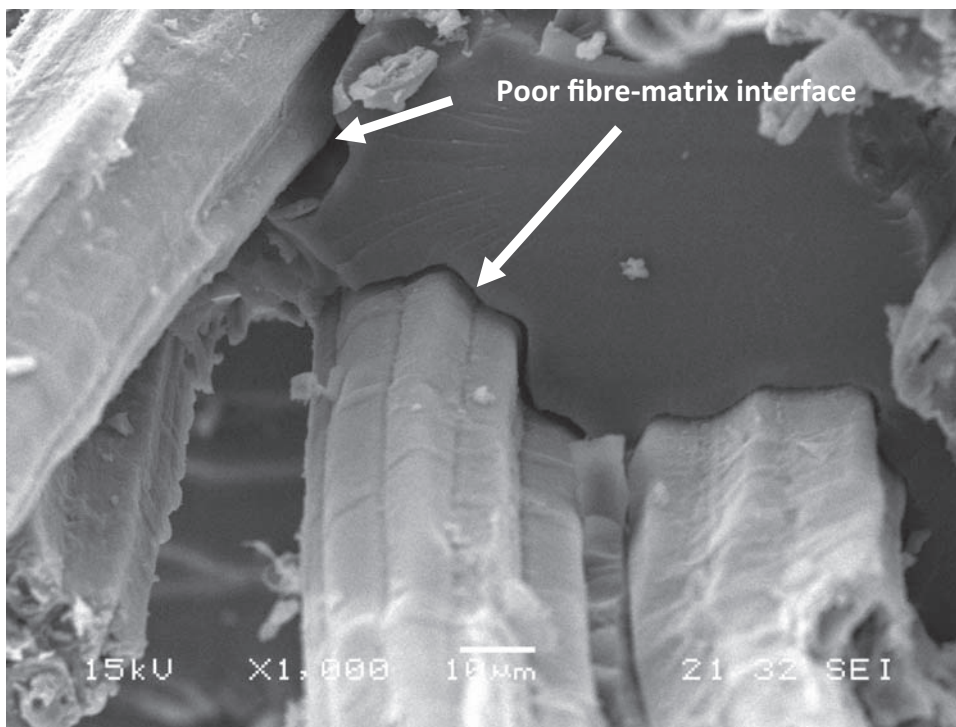


**Figure 2.** SEM micrograph of synthetic vinylester reinforced jute fibre biocomposite.  
SEM: scanning electron microscopy.

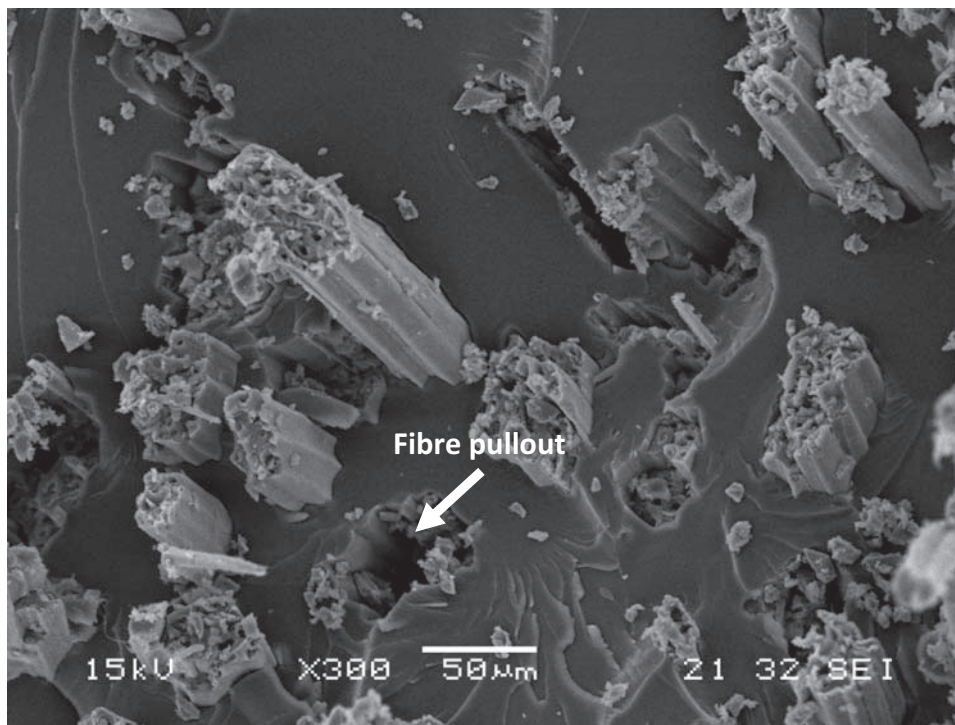


**Figure 3.** SEM micrograph of 50/50 vinyl ester/AEHO reinforced jute fibre biocomposite. SEM: scanning electron microscopy; AEHO: acrylated epoxidized hemp oil.

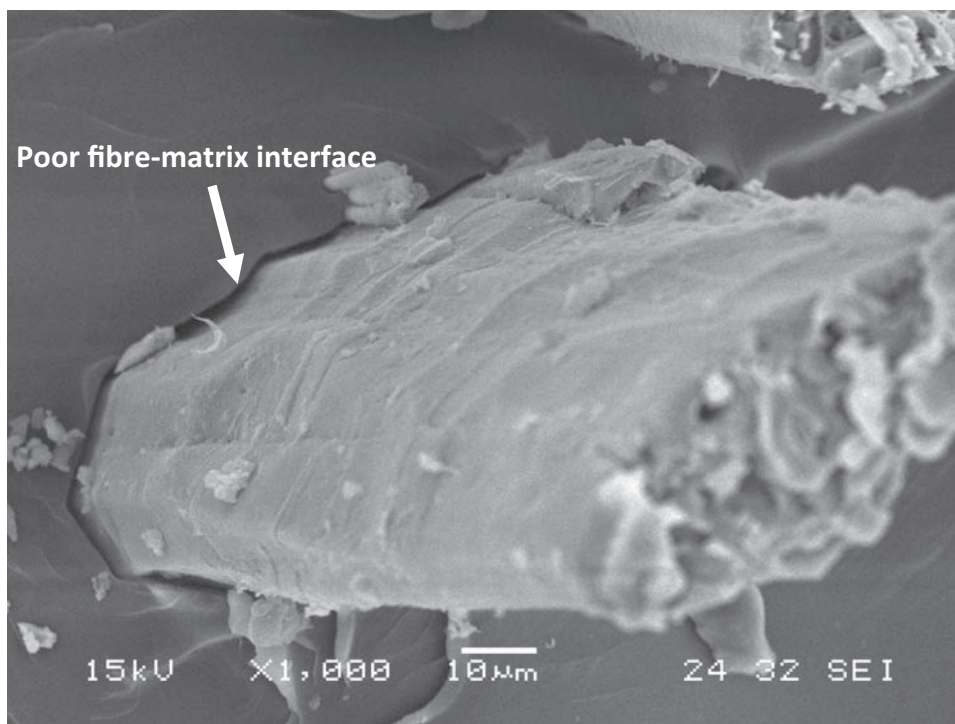


**Figure 4.** SEM micrograph of 50/50 vinyl ester/AEHO reinforced jute fibre biocomposite. SEM: scanning electron microscopy; AEHO: acrylated epoxidized hemp oil.



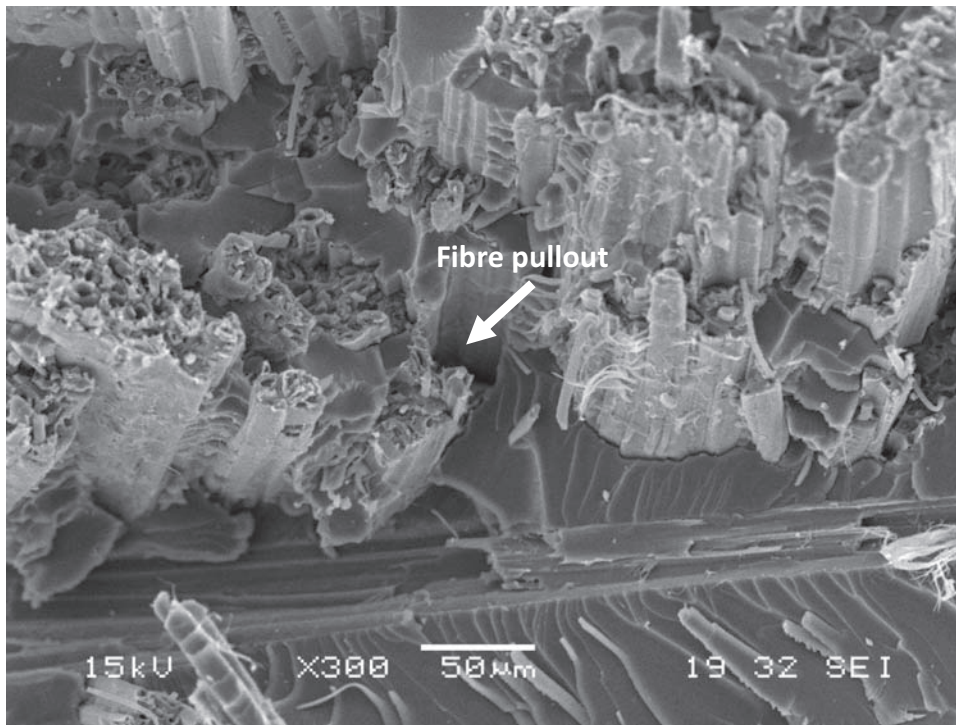


**Figure 5.** SEM micrograph of AEHO reinforced jute fibre biocomposite.  
SEM: scanning electron microscopy; AEHO: acrylated epoxidized hemp oil.

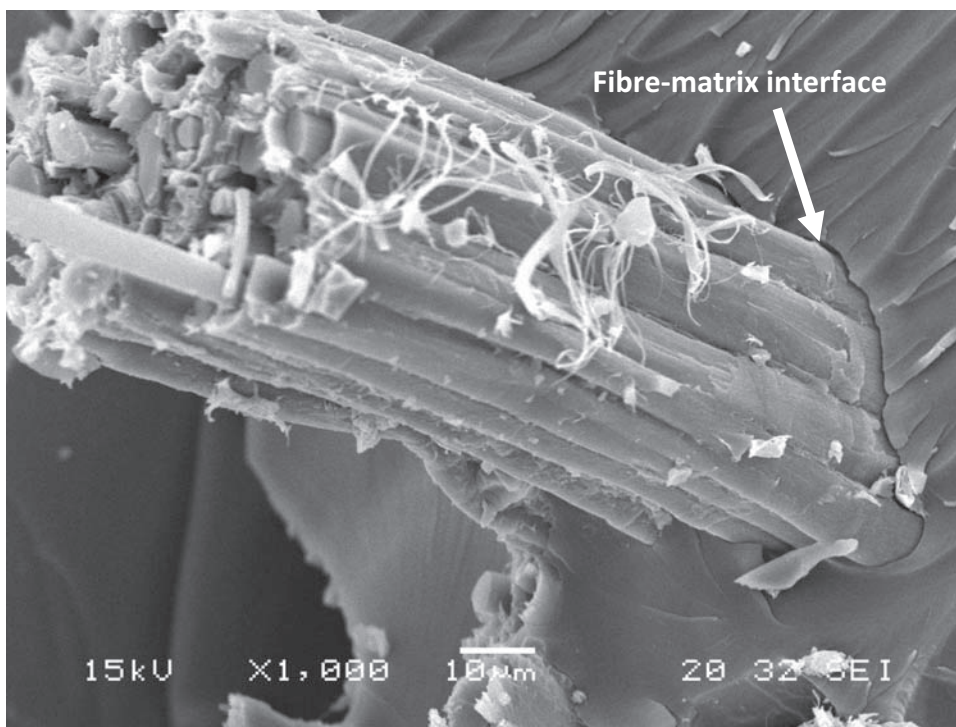


**Figure 6.** SEM micrograph of AEHO reinforced jute fibre biocomposite.  
SEM: scanning electron microscopy; AEHO: acrylated epoxidized hemp oil.

**Table 1.** Mechanical properties of AEHO-based bioresins and biocomposites.

Sample type	ILSS (MPa)	Flexural strength (MPa)	Flexural modulus (MPa)	Tensile strength (MPa)	Young's modulus (MPa)	Charpy impact (kJ/m <sup>2</sup> )
<b>Neat bioresin</b>						
VE	–	85.27 ± 6.82	2364 ± 186	–	–	–
50/50 (VE/AEHO)	–	61.58 ± 13.01	1627 ± 264	–	–	–
AEHO	–	36.83 ± 0.84	744 ± 112	–	–	–
<b>Biocomposite</b>						
VE	3.28 ± 0.61	53.92 ± 2.31	3402 ± 230	31.80 ± 1.53	3903 ± 207	10.60 ± 1.80
50/50 (VE/AEHO) + JF	4.41 ± 0.91	51.89 ± 1.43	3145 ± 528	26.27 ± 3.27	3772 ± 422	11.40 ± 2.24
AEHO + JF	4.70 ± 0.52	48.63 ± 1.39	2791 ± 116	25.17 ± 4.79	3515 ± 231	12.20 ± 3.95

AEHO: acrylated epoxidized hemp oil; ILSS: interlaminar shear strength; VE: vinyl ester; JF: jute fibre.

adhesion of the 100% AEHO-based samples is due to surface chemical compatibility between the natural fibres and the bioresin. Moreover, Kabir et al.<sup>14</sup> reasons that the presence of hemicelluloses and lignin present on the untreated fibre surface causes a reduction in composite performance through reduced stress transfer efficiency. Specifically the interaction of the reactive hydroxyl groups on the fibre surface with the matrix is impeded. It is theorised that the greater quantity of hydroxyl groups are present in the AEHO bioresin compared to the VE contributing to enhanced fibre–matrix adhesion. These hydroxyl functional groups present in the AEHO serve to interact with the hydroxyl groups present in the cellulose of the natural fibres to form strong hydrogen bonds thereby improving adhesion and ultimately flexural and ILSS performance. Therefore as a result of these findings it is expected that ILSS will be higher for samples containing AEHO compared with those based on VE. By utilising chemical treatments on the natural fibres improvements in fibre–matrix interfacial adhesion would be expected.<sup>4,14–21</sup>

### Mechanical properties

Table 1 summarises all of the mechanical testing results. It was found that AEHO and 50/50 samples displayed higher ILSS than VE-based samples with 100% AEHO-based samples displaying the highest ILSS. As the flexural properties of the VE neat resin is superior to those of the AEHO systems, these results suggest that the fibre–matrix interfacial adhesion is stronger for the AEHO-based samples compared with the VE-based samples. This was confirmed by SEM analysis whereby it was apparent that AEHO-based samples exhibited improved fibre–matrix interfacial adhesion compared with VE-based samples. Accordingly, as previously mentioned the surface chemical compatibility

between the natural fibres and the bioresin, specifically the greater quantity of hydroxyl groups present in the AEHO bioresin when compared to the VE is proposed as the reason for enhanced fibre–matrix adhesion. The greater quantity of hydroxyl functional groups present in the AEHO serve to interact with the hydroxyl groups present in the cellulose of the natural fibres to form strong hydrogen bonds thereby improving adhesion and ultimately ILSS.

VE resin was found to display higher flexural stress compared with the AEHO-based bioresin samples. Specifically neat VE resin samples exhibited approximately 1.5–3 times the flexural strength of AEHO-based samples. This behaviour was anticipated and is attributed to the long fatty acid chains of the AEHO in a similar manner to EHO imparting flexibility to the matrix. In terms of biocomposite properties it was observed that the addition of jute fibre reinforcement resulted in an increase in flexural strength for only the 100% AEHO-based sample. Both the VE and the 50/50 (VE/AEHO) samples displayed a reduction in flexural strength with the addition of fibre reinforcement. This apparent reduction in flexural strength is attributed to poor fibre–matrix interfacial adhesion for these samples and is supported by the SEM images and ILSS results. As a result of this behaviour the overall flexural strength of all three composite systems is similar in nature and is within 10% difference. The flexural modulus of AEHO-based neat bioresin and biocomposite samples are shown in Figure 5.<sup>22</sup> The neat commercial VE resin displayed almost 1.45 and 3.2 times the flexural modulus of the 50/50 and AEHO bioresin samples. The addition of the jute fibre reinforcement to the matrices was found to greatly improve the flexural modulus for all sample types. Improvements in flexural modulus were found to be in the order of 1.43, 1.93 and 3.75 for the VE, 50/50 and AEHO-based biocomposite samples, respectively.



Due to this reinforcement and improvement in flexural modulus, the 50/50 and AEHO-based samples displayed flexural moduli that were only approximately 8% and 18% lower than the commercial VE-based sample, respectively.

In terms of flexural properties of neat bioresins there is limited literature available. However, Grishchuk and Karger-Kocsis<sup>22</sup> reported the flexural properties of VE/AESO blends. Daron-XP-45-A2 VE was blended with commercial AESO in concentrations of 100/0, 75/25, 50/50 and 25/75 VE/AESO. The neat VE displayed a flexural modulus and strength of 3212 and 123 MPa, respectively. Reductions in flexural properties were observed with increased AESO concentration with the 50/50 displaying a flexural modulus and strength of 1516 MPa and 61 MPa, respectively. In comparison the 25/75 sample exhibited a flexural modulus and strength of 234 MPa and 15 MPa, respectively. It is worth noting, however, that in this study styrene was not added to the AESO. In a United States patent awarded to Wool et al.<sup>23</sup> the flexural modulus of AESO prepared in the ratio 100:45:5 (AESO: styrene: divinyl benzene) was reported as 723 MPa. In comparison the AEHO presented herein is similar with a flexural modulus of 744 MPa. Lu and Wool<sup>24</sup> produced AELO from a commercially available ELO and obtained a flexural modulus and strength of 2.31 GPa and 78.73 MPa. The high level of epoxides per triglyceride, on average 6.2 resulted in a high number of acrylate groups per triglyceride, approximately 5.7–5.8 thereby resulting in a highly crosslinked, stiff polymer.

Morye and Wool<sup>13</sup> studied the mechanical properties of glass/flax fibre reinforced AESO-based biocomposites. In terms of flexural performance for the 100% flax reinforced samples they obtained flexural modulus and strength of 3.8 GPa and 61 MPa, respectively. Fibre wt% was stated as being between 31% and 40%. Williams and Wool<sup>25</sup> also characterised the mechanical properties of AESO flax fibre reinforced biocomposites in a similar study. Fibre wt% ranged from 20% to 40% with flexural modulus varying from 2.7 GPa to a maximum of 4.2 GPa at 35 wt%. Comparing these results with those obtained for AEHO reinforced jute fibre samples as studied within, it is noted that flexural modulus is comparable for both systems. Similar results were found for the flexural strength whereby at 25 wt% flexural strength was found to be approximately the same as those AEHO reinforced jute fibre samples study herein.

It can be observed that VE-based samples exhibit the highest tensile strength with the addition of AEHO resulting in decreased performance. In terms of Young's modulus all three samples are within 10% of each other. Therefore given the standard deviation (as pictured from the error bars) it is not unreasonable to

state that all three sample types offer similar tensile performance, both in terms of Young's modulus and strength. It is presented that a plausible reason for this similar performance is due to the poor compatibility of the VE with the natural fibre reinforcement. Similarities in performance were also noted in terms of flexural properties. Through the addition of natural fibre reinforcement the AEHO-based samples exhibit superior fibre–matrix adhesion than VE-based samples as shown in the SEM images.

Morye and Wool<sup>13</sup> studied the mechanical properties of glass/flax fibre reinforced AESO-based biocomposites. In terms of tensile performance for the 100% flax reinforced samples they obtained a Young's modulus and strength of 2 GPa and 31.8 MPa, respectively. Fibre wt% was stated as being between 31% and 40%. Williams and Wool<sup>25</sup> also characterised the mechanical properties of AESO flax fibre reinforced biocomposites in a similar study. Fibre wt% ranged from 20% to 40% with Young's modulus varying from approximately 3.1 GPa to a maximum of 4.7 GPa at 40 wt%. Comparing these results with those obtained for AEHO reinforced jute fibre samples as studied within, it is noted that Young's modulus is comparable for both systems. Similar results were found for the tensile strength whereby at 25 wt% tensile strength was found to be marginally lower than the AEHO reinforced jute fibre samples study herein.

Charpy impact strength for all three samples was found to be similar in nature, especially accounting for the standard deviation. The impact strength of the vinylester resin was expected to be lower than that of the acrylated AEHO-based bioresins, since the former is much less flexible, as shown in Table 1. However, according to the SEM analysis the fibre–matrix interfacial adhesion of the AEHO-based samples was observed to be improved when compared with that of the VE sample. Therefore these two seemingly opposite effects could be responsible for the impact properties of all samples having similar performance.

### Dynamic mechanical properties

Figures 7 and 8 and Table 2 outline the visco-elastic behaviour of the AEHO-based bioresins and biocomposites in terms of the storage modulus and  $\tan \delta$  as a function of temperature. Table 2 further illustrates the storage modulus at 40°C,  $T_g$  and crosslink density. For all bioresin and biocomposite systems the storage modulus,  $T_g$  and crosslink density were found to decrease with the addition of AEHO. As expected VE systems displayed the highest properties of all systems. The addition of jute fibre reinforcement resulted in improved storage modulus ranging from approximately 34% for the VE sample through to a maximum of

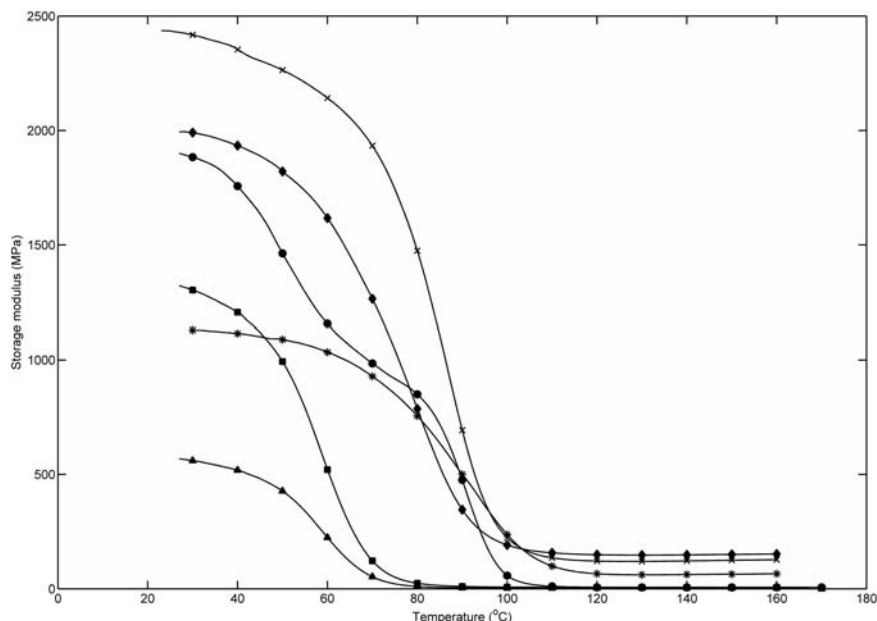


**Figure 7.** Storage modulus versus temperature; VE + JF (x), 50/50 + JF (◆), AEHO + JF (\*), VE (●), 50/50 (■), AEHO (▲). VE: vinyl ester; JF: jute fibre; AEHO: acrylated epoxidized hemp oil.

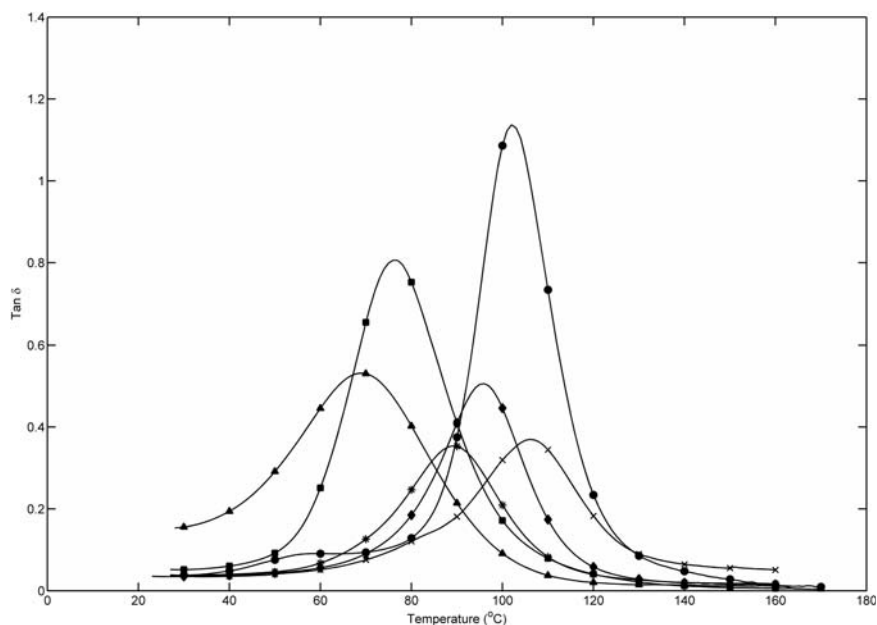


**Figure 8.** Tan  $\delta$  versus temperature; VE + JF (x), 50/50 + JF (◆), AEHO + JF (\*), VE (●), 50/50 (■), AEHO (▲). VE: vinyl ester; JF: jute fibre; AEHO: acrylated epoxidized hemp oil.

215% for the AEHO sample. This behaviour is in agreement with the trends observed for the flexural properties of the biocomposites compared with the neat bioresin samples whereby AEHO samples displayed a larger increase in flexural modulus compared with VE-based samples.

In terms of  $T_g$  the VE systems showed the highest values with reductions being apparent for AEHO-based systems. The addition of fibre reinforcement resulted in a marginal increase in  $T_g$  for the VE system from 102°C to 106°C. Both AEHO-based systems realised an increase in  $T_g$  of 25% and 28% from the neat bioresin

**Table 2.** Dynamical mechanical properties of AEHO-based bioresins and biocomposites.

Sample type	Storage modulus at 40°C (MPa)	$T_g$ (°C)	Crosslink density (mol/m <sup>3</sup> )
Neat bioresin			
VE	1757	102	6654
50/50	1206	76	6542
AEHO	519	68	4301
Biocomposite			
VE + JF	2354	106	13,965
50/50 + JF	1934	95	13,327
AEHO + JF	1115	87	12,861

AEHO: acrylated epoxidized hemp oil; VE: vinyl ester; JF: jute fibre.

**Table 3.** Moisture absorption properties of AEHO-based bioresins and biocomposites.

Sample type	Diffusion coefficient $\times 10^{-6}$ (mm <sup>2</sup> /s)	Saturation moisture content (%)
Neat bioresin		
VE	0.801	0.52
50/50 (VE/AEHO)	0.847	0.73
AEHO	0.958	0.80
Biocomposite		
VE	8.81	4.01
50/50 (VE/AEHO)	9.54	4.94
AEHO	10.90	6.30

AEHO: acrylated epoxidized hemp oil; VE: vinyl ester.

samples. The  $\tan \delta$  peaks of the AEHP-based samples were found to become broader when compared with the VE sample. This was also found to be the case for AESO/VE systems as studied by Grishchuk and Karger-Kocis.<sup>22</sup> No peak doubling was found to occur for the 50/50 sample indicating satisfactory compatibility between the VE and AEHO resins. In a study of VE/AESO blends Grishchuk and Karger-Kocis<sup>22</sup> found that  $T_g$  also decreased with increased AESO. Compared to the observed storage modulus of the neat AEHO sample Lu and Wool<sup>24</sup> and Khot et al.<sup>26</sup> found the storage moduli of AESO with 40 wt% styrene and AELO with 33 wt% styrene to be in the order of 1.3 GPa and approximately 2 GPa, respectively. Furthermore they also reported  $T_g$  values of 79°C for

the AESO and approximately 105°C for the AELO neat resin samples.

Crosslink densities were also found to decrease with the addition of AEHO. As anticipated the VE-based samples displayed the highest crosslink densities among all other samples. The crosslink density of the neat VE system was found to be almost twice that of the neat AEHO sample. When fibre reinforcement was added the crosslink densities were found to dramatically increase similar to those reported above for the EHO-based systems. Accordingly this behaviour is primarily due to the higher storage moduli of the biocomposites compared with the neat bioresins. It is also interesting to note that the biocomposite samples displayed similar crosslink densities with data spread being less than 10%. Given the similarity in crosslink densities for the biocomposites it is reasoned that the greater quantity of hydroxyl groups in the AEHO bioresin when compared to the VE are responsible for the crosslinking of the end biocomposites. Consequently the final result is a greater improvement in crosslink density for the AEHO-based samples compared with that obtained from the VE samples.

In comparison to the crosslink densities found in this study, Lu and Wool<sup>24</sup> determined the crosslink density for AELO to be 5050 mol/m<sup>3</sup>. Indeed it is expected that AEHO would have a lower crosslink density than AELO due to having less acrylates per triglyceride. Campanella et al.<sup>27</sup> observed that the crosslink density of AESO resins was influenced by the styrene content. Moreover, it was observed that crosslink densities ranged from 3700 to 2100 mol/m<sup>3</sup> for AESO samples containing no styrene through to 35 wt%. In a study to determine properties of an AESO-based material intended to be used in the PCB industry, Zhan and Wool<sup>28</sup> determined the crosslink density of AESO polymers containing 30 wt% styrene and 0–15 wt% of DB. Crosslink densities were found to increase with DB content from 1833 to a maximum of 7133 mol/m<sup>3</sup> at 15 wt% DB.

### Moisture absorption

The water absorption results obtained in this work showed that the composites immersed in distilled water at 23.1°C followed a linear Fickian behaviour, whereby the moisture weight gains gradually reached equilibrium after a rapid initial phase. Akil et al.<sup>29</sup> mentioned three different mechanisms acting in the water absorption of fibre reinforced composites, namely diffusion of water molecules inside the micro gaps between polymer chains, capillary transport into the gaps and flaws of the interfaces between fiber and the matrix and transport through microcracks in the matrix arising from the fibre swelling (particularly in the case of



natural fibre composites). Moreover, the hydrophilic temperament of natural fibres increases water absorption of the final composites.

Table 3 summarises the moisture absorption behaviour of the AEHO-based neat resin and biocomposite samples. From examining the data it is apparent that increasing AEHO content results in increasing saturation moisture content and diffusion coefficient. As expected, the highest water absorption was shown by the jute fibre samples. These fibres dramatically increase both the diffusion coefficient and saturation moisture content of the composites as they absorb water as a consequence of their hydrophilic nature given by the hydroxyl groups in the cellulose component of the fibres and swell, allowing the transport of water along microcracks in the matrix arising from the swelling of fibers.<sup>13</sup> Through the addition of fibre reinforcement the saturation moisture content increased approximately by a factor of approximately 6.75–8. Similarly the diffusion coefficients increased by a factor of approximately 11.

## Conclusions

AEHO-based bioresins and jute fibre reinforced biocomposites were manufactured and compared with VE-based samples in terms of SEM, mechanical, dynamic mechanical and water absorption properties. ILSS was found to increase with increasing AEHO content suggesting that the fibre–matrix interfacial adhesion is stronger for the AEHO-based samples compared with the VE-based samples. This was confirmed to be the case with SEM analysis. In terms of flexural performance the flexural strength of the neat bioresins were found to be higher than those of the biocomposite samples. The VE-based neat resin samples showed markedly higher flexural stress than samples containing AEHO. However, when jute fibre reinforcement was incorporated, all three systems exhibited similar flexural performance. Flexural modulus was found to increase for all three biocomposite types over the bioresin samples. This was expected due to the addition of the relatively brittle jute fibres. VE samples displayed the highest flexural moduli for both neat bioresin and biocomposite samples; however, the difference was marginal in the case of the biocomposites. AEHO-based jute reinforced biocomposites were subjected to tensile tests. It was observed that VE-based samples exhibited the highest tensile strength with the addition of AEHO resulting in a slight reduction in performance. Young's modulus was found to be similar for all three sample types Charpy impact properties of all three samples were similar in nature, especially accounting for the standard deviation.

DMA was performed in order to characterise the visco-elastic behaviour of the AEHO-based bioresins and biocomposites. Specifically VE-based samples were found to have higher  $T_g$ , storage modulus and crosslink density than AEHO-based samples. As the AEHO content increased  $T_g$ , storage modulus and crosslink density were found to decrease. The addition of jute fibre reinforcement resulted in a marginal increase in  $T_g$ , for the VE samples; however, a noticeable increase was observed for AEHO-based samples. Similarly to the EHO/ESO samples the crosslink density was found to significantly increase with the addition of jute fibre reinforcement. In studying the moisture absorption of AEHO-based bioresins and biocomposites it was found that increasing AEHO content resulted in increasing saturation moisture content and diffusion coefficient. Also as previously found with the EHO-based samples, overall the moisture absorption was heavily dominated by fibre addition rather than resin type.

## Funding

The authors would like to thank the Queensland State Government for providing a Smart Futures PhD Scholarship, the Australian Government for providing an Endeavour Research Award, and the National Scientific and Technical Research Council of Argentina (CONICET), which provided financial support for this research work.

## Conflict of interest

None declared.

## Acknowledgement

The authors extend their thanks to Mr Wayne Crowell for providing technical support.

## References

- Mishra HK, Dash BN, Tripathy SS, et al. A study on mechanical performance of jute-epoxy composites. *Polym-Plast Technol Eng* 2000; 39(1): 187–198.
- Ray D, Sarkar BK and Bose NR. Impact fatigue behaviour of vinylester resin matrix composites reinforced with alkali treated jute fibres. *Compos Part A: Appl Sci Manuf* 2002; 33(2): 233–241.
- Datta C, Basu D and Banerjee A. Mechanical and dynamic mechanical properties of jute fibers–Novolac–epoxy composite laminates. *J Appl Polym Sci* 2002; 85(14): 2800–2807.
- Tripathy SS, Di Landro L, Fontanelli D, et al. Mechanical properties of jute fibers and interface strength with an epoxy resin. *J Appl Polym Sci* 2000; 75(13): 1585–1596.
- Dash BN, Rana AK, Mishra HK, et al. Novel, low-cost jute-polyester composites. Part 1: Processing, mechanical properties, and SEM analysis. *Polym Compos* 1999; 20(1): 62–71.

6. Gassan J and Bledzki AK. Possibilities for improving the mechanical properties of jute/epoxy composites by alkali treatment of fibres. *Compos Sci Technol* 1999; 59(9): 1303–1309.
7. Jústiz-Smith NG, Virgo GJ and Buchanan VE. Potential of Jamaican banana, coconut coir and bagasse fibres as composite materials. *Mater Charact* 2008; 59(9): 1273–1278.
8. Mohanty AK and Misra M. Studies on jute composites—a literature review. *Polym-Plast Technol Eng* 1995; 34(5): 729–792.
9. Francucci G, Cardona F and Manthey NW. Cure kinetics of an acrylated epoxidized hemp oil-based bioresin system. *J Appl Polym Sci* 2012; 128(3): 2030–2037.
10. Manthey NW, Cardona F, Francucci G, et al. Green building materials: hemp oil based biocomposites. *International conference on architectural and civil engineering*. Bali, Indonesia, 2012, pp.827–83324–25 October 2012.
11. Shabeer A, Chandrashekhara K and Schuman T. Synthesis and characterization of soy-based nanocomposites. *J Compos Mater* 2007; 41(15): 1825–1849.
12. Miyagawa H, Mohanty A, Misra M, et al. Thermo-physical and impact properties of epoxy containing epoxidized linseed oil-amine-cured epoxy. *Macromol Mater Eng* 2004; 289(7): 636–641.
13. Morye SS and Wool RP. Mechanical properties of glass/flax hybrid composites based on a novel modified soybean oil matrix material. *Polym Compos* 2005; 26(4): 407–416.
14. Kabir MM, Wang H, Lau KT, et al. Mechanical properties of chemically-treated hemp fibre reinforced sandwich composites. *Compos Part B: Eng* 2012; 43(2): 159–169.
15. George J, Sreekala MS and Thomas S. A review on interface modification and characterization of natural fiber reinforced plastic composites. *Polym Eng Sci* 2001; 41(9): 1471–1485.
16. Le Troedec M, Sedan D, Peyratout C, et al. Influence of various chemical treatments on the composition and structure of hemp fibres. *Compos Part A: Appl Sci Manuf* 2008; 39(3): 514–522.
17. Li X, Tabil L and Panigrahi S. Chemical treatments of natural fiber for use in natural fiber-reinforced composites: a review. *J Polym Environ* 2007; 15(1): 25–33.
18. Mehta G, Drzal LT, Mohanty AK, et al. Effect of fiber surface treatment on the properties of biocomposites from nonwoven industrial hemp fiber mats and unsaturated polyester resin. *J Appl Polym Sci* 2006; 99(3): 1055–1068.
19. Rong MZ, Zhang MQ, Liu Y, et al. The effect of fiber treatment on the mechanical properties of unidirectional sisal-reinforced epoxy composites. *Compos Sci Technol* 2001; 61(10): 1437–1447.
20. Thomsen AB, Thygesen A, Bohn V, et al. Effects of chemical-physical pre-treatment processes on hemp fibres for reinforcement of composites and for textiles. *Ind Crops Prod* 2006; 24(2): 113–118.
21. Valadez-Gonzalez A, Cervantes-Uc JM, Olayo R, et al. Effect of fiber surface treatment on the fiber-matrix bond strength of natural fiber reinforced composites. *Compos Part B: Eng* 1999; 30(3): 309–320.
22. Grishchuk S and Karger-Kocsis J. Hybrid thermosets from vinyl ester resin and acrylated epoxidized soybean oil (AESO). *eXPRESS Polym Lett* 2010; 5(1): 2–11.
23. Wool R, Kusefoglu S, Palmese G, et al. High modulus polymers and composites from plant oils. Patent 6121398, USA, 2000.
24. Lu J and Wool RP. Novel thermosetting resins for SMC applications from linseed oil: synthesis, characterization, and properties. *J Appl Polym Sci* 2006; 99(5): 2481–2488.
25. Williams GI and Wool RP. Composites from natural fibers and soy oil resins. *Appl Compos Mater* 2000; 7(5): 421–432.
26. Khot SN, Lascala JJ, Can E, et al. Development and application of triglyceride-based polymers and composites. *J Appl Polym Sci* 2001; 82(3): 703–723.
27. Campanella A, La Scala JJ and Wool RP. The use of acrylated fatty acid methyl esters as styrene replacements in triglyceride-based thermosetting polymers. *Polym Eng Sci* 2009; 49(12): 2384–2392.
28. Zhan M and Wool RP. Biobased composite resins design for electronic materials. *J Appl Polym Sci* 2010; 118(6): 3274–3283.
29. Akil HM, Cheng LW, Mohd Ishak ZA, et al. Water absorption study on pultruded jute fibre reinforced unsaturated polyester composites. *Compos Sci Technol* 2009; 69(11–12): 1942–1948.